

NOTICE

1

NOTICE
 This report was prepared as an account of work sponsored by the United States Government. Neither the United States nor the United States Energy Research and Development Administration, nor any of their employees, nor any of their contractors, subcontractors, or their employees, makes any warranty, express or implied, or assumes any legal liability or responsibility for the accuracy, completeness or usefulness of any information, apparatus, product or process disclosed, or represents that its use would not infringe privately owned rights.

PORTIONS OF THIS REPORT ARE ILLEGIBLE. It has been reproduced from the best available copy to permit the broadest possible availability.

METALLURGICAL CONSIDERATIONS IN THE PRODUCTION AND USE OF FeTi ALLOYS FOR HYDROGEN STORAGE

G.D. Sandrock

The International Nickel Company, Inc., Paul D. Merica Research Laboratory, Suffern, NY 10901

J.J. Reilly and J.R. Johnson

Brookhaven National Laboratory, Department of Applied Science, Upton, NY 11973

Conf-760906-12

Abstract

Hydriding alloys based on the intermetallic compound FeTi have potential for the safe and convenient storage of hydrogen, both for mobile and stationary applications. Optimum technical and economic use of these alloys requires an understanding of the physical metallurgy of the system and its relation to the hydriding behavior. This paper provides an introduction to some of the metallurgical factors that affect hydriding behavior in FeTi and related alloys. Properties considered are hydrogen storage capacity, activation, decrepitation (particle size breakdown) and hydride stability (dissociation pressure).

INTRODUCTION

The hydriding and dehydriding properties of the intermetallic compound FeTi were first reported in detail by Reilly and Wiswall of BNL early in 1974[1]. Since that time FeTi (and its modifications) has been widely recognized as a prime candidate for the safe and convenient temporary storage of hydrogen as a rechargeable metal hydride. Several prototype vehicles have been built using FeTi hydride as a hydrogen fuel carrier[2-5], along with a small demonstration model of a BNL developed electric peak shaving system that utilizes a hydrogen cycle and FeTi hydride storage[6]. Both of these applications, among many other possibilities, suggest a widespread future use of FeTi, and its modifications, in the area of hydrogen energy.

As with any other engineering alloy, the optimum production and use of FeTi for hydrogen storage requires an understanding of its physical metallurgy. With the exception of some preliminary studies recently presented by Pick and Wenzl[7], virtually nothing on this subject has appeared for FeTi in the open literature. In the present paper, we briefly discuss some of our studies to define the metallurgy of FeTi and its relationship to the hydriding behavior. In particular we will consider the following hydriding properties of engineering interest: (a) hydrogen storage capacity, (b) activation, (c) decrepitation (particle size breakdown), and (d) hydride stability (i.e., dissociation pressure at a given temperature). To be sure, there are other properties of engineering interest, such as heats of reaction, hydriding kinetics, thermal conductivity and poisoning, that can be related to metallurgy, but information in these areas is very preliminary at present. More details of these studies will be presented later along with extensive studies of alloy melting techniques[8].

EXPERIMENTAL TECHNIQUES USED

A variety of standard metallography and metal physics techniques were used to characterize FeTi, and ternary alloys, in the virgin (as-cast), partially hydrided, and hydrided/dehydrided conditions. The principal techniques used included the following:

1. Optical metallography, where solid samples or powder particles are polished in cross section and etched to observe the microstructure under a metallurgical (reflected light) microscope. The etchant used was $82\text{H}_2\text{O}-14\text{HNO}_3-4\text{HF}$, by volume.
2. Electron microprobe analysis, which provides quantitative chemical analyses of individual phases on a microscale.
3. X-ray diffraction, which provides crystal structure (lattice parameter) information as well as aiding in minor phase identification. Diffractometer techniques were used.

In addition some use was made of scanning electron microscopy (particle sizes and shapes) and scanning Auger spectroscopy (surface chemistry).

Alloy samples of various purities were prepared by a variety of techniques, including consumable and non-consumable electrode inert gas arc melting, vacuum induction melting and air induction melting. Contaminants such as oxygen, nitrogen and carbon were studied. These originated from raw materials, crucibles, or melting atmospheres. Elements such as manganese, chromium, nickel or vanadium were purposely added to high purity arc melts to study substitution effects.

Hydriding data were obtained using equipment and techniques similar to those described earlier[1]. Ultra-high purity grade (99.999%) hydrogen was used. Partially hydrided samples were prepared by allowing activation to proceed to partial completion and then cooling the sample to liquid nitrogen temperature. This allowed the hydrogen above the sample to be evacuated and the reaction chamber to be backfilled with air, thus "stabilizing" the hydride and allowing the partially hydrided samples to be prepared by conventional metallographic techniques.

HYDROGEN STORAGE CAPACITY

The storage capacity of FeTi is intimately related to the metallurgy and microstructure of Fe-Ti alloys. The capacity is related predominantly to two factors: (a) the Fe/Ti ratio and (b) the alloy oxygen content.

The effect of Fe/Ti ratio is straightforward and can be easily seen from the Fe-Ti binary phase diagram (Figure 1). The FeTi phase exists over a

MASTER

CONTRACT NO. E(30-1)-16
 DISTRIBUTION OF THIS DOCUMENT IS UNLIMITED

SAC

DISCLAIMER

This report was prepared as an account of work sponsored by an agency of the United States Government. Neither the United States Government nor any agency Thereof, nor any of their employees, makes any warranty, express or implied, or assumes any legal liability or responsibility for the accuracy, completeness, or usefulness of any information, apparatus, product, or process disclosed, or represents that its use would not infringe privately owned rights. Reference herein to any specific commercial product, process, or service by trade name, trademark, manufacturer, or otherwise does not necessarily constitute or imply its endorsement, recommendation, or favoring by the United States Government or any agency thereof. The views and opinions of authors expressed herein do not necessarily state or reflect those of the United States Government or any agency thereof.

DISCLAIMER

Portions of this document may be illegible in electronic image products. Images are produced from the best available original document.

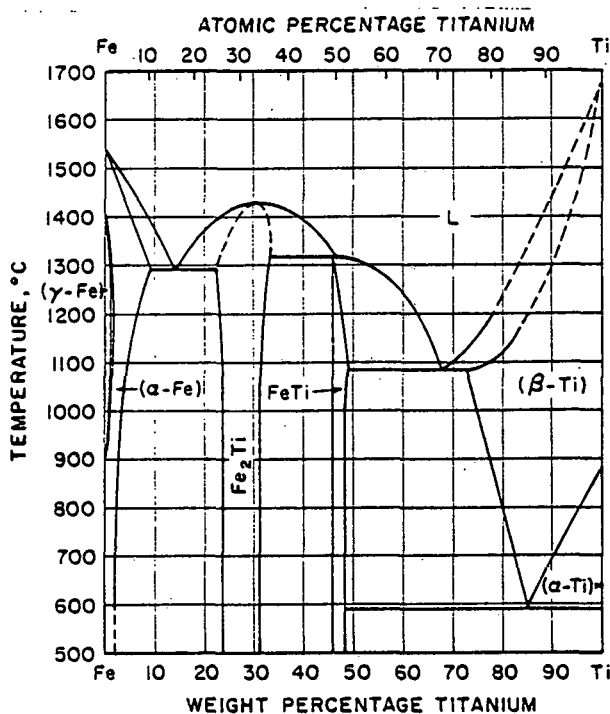


FIGURE 1 - Fe-Ti PHASE DIAGRAM. (AFTER REF. 9)

narrow ($\sim 2.5\%$) composition range near the center of the phase diagram. If the prepared composition is only slightly deficient in Ti (~ 49.5 at. % Ti) the two-phase FeTi + Fe₂Ti field is entered. Fe₂Ti is not known to form a hydride and is useless for H₂ storage purposes. It simply reduces the amount of the FeTi phase and lowers the overall capacity. On the other hand if slightly excess Ti is present (~ 52 at. % Ti) the two-phase FeTi + Ti solid solution (β - or α -Ti) field is entered. β - or α -Ti hydrides readily form on the first cycle; however, it forms a very stable hydride that is not readily reversible at the near-ambient temperatures of interest for FeTi. Thus the amount of Ti solid solution phase should also be minimized. The production target then is to aim for the maximum amount of FeTi phase by controlling the composition as close as possible to 49.5-52 at. % Ti range. In practice this is fairly easy to achieve.

The deleterious effect of oxygen contamination on storage capacity is more complicated and more difficult to control. Molten FeTi has a strong affinity for oxygen. It readily getters oxygen from the air and, more seriously, from common oxide crucibles. Table I shows the degree of melt contamination that can occur during vacuum induction melting with three common crucibles. The numerical results shown in Table I should be considered approximate because they represent only

Table I

Effect of Crucible on Melt Contamination During Vacuum Induction Melting Of FeTi

Crucible Material	O-Contamination, wt. %	M-Contamination, wt. %
MgO	0.072	<0.001Mg
Al ₂ O ₃	1.14	1.23Al
ZrO ₂	0.30	0.45Zr

one trial each. During melting, Ti was added quickly as possible ($\sim 8-10$ min) and the melt immediately poured; nevertheless, substantial crucible attack still occurred. In addition to melt contamination, the extremely poor crucible life would raise the production cost of the alloy. In spite of the relatively low contamination from MgO crucibles, severe degradation of the crucible still occurred.

The effect of oxygen content on the hydriding curve (40°C desorption isotherm) is shown in Figure 2. While the lower plateau level and

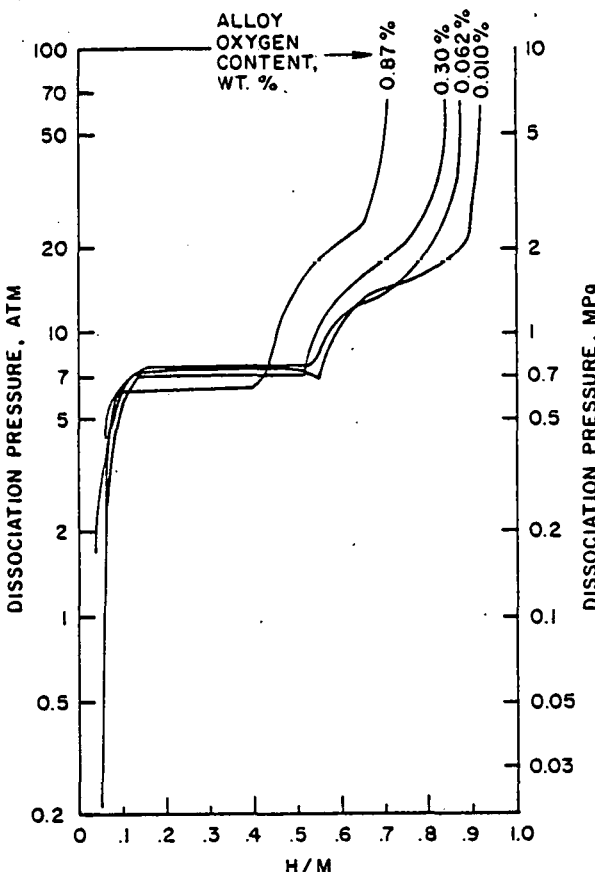


FIGURE 2 - EFFECT OF ALLOY OXYGEN CONTENT ON THE 40°C HYDROGEN DESORPTION ISOTHERM OF FeTi.

general curve shape is not significantly affected by O-content, the maximum H-level is substantially reduced. The reason for this can be seen in the alloy microstructure. The microstructures of fairly low-O FeTi (0.062 wt. %) and intermediate-O FeTi (0.30 wt. %) are shown in Figure 3. The Fe/Ti ratios of these alloys are within the single phase range of Figure 1, but they are far from being single phase alloys. A second phase is invariably seen with the amount of that second phase increasing with increasing oxygen content. At low oxygen content (Figure 3a) the phase takes a fine "eutectic" distribution. At higher O-contents there are larger "primary" crystals of the phase in addition to the fine eutectic particles.

Electron microprobe and x-ray diffraction studies indicated that the phase is an oxygen stabilized phase of the approximate composition Fe₇Ti_{1.0}O₃. The composition of the phase varies somewhat around this stoichiometry. There is also evidence of minor amounts of another O-rich phase,

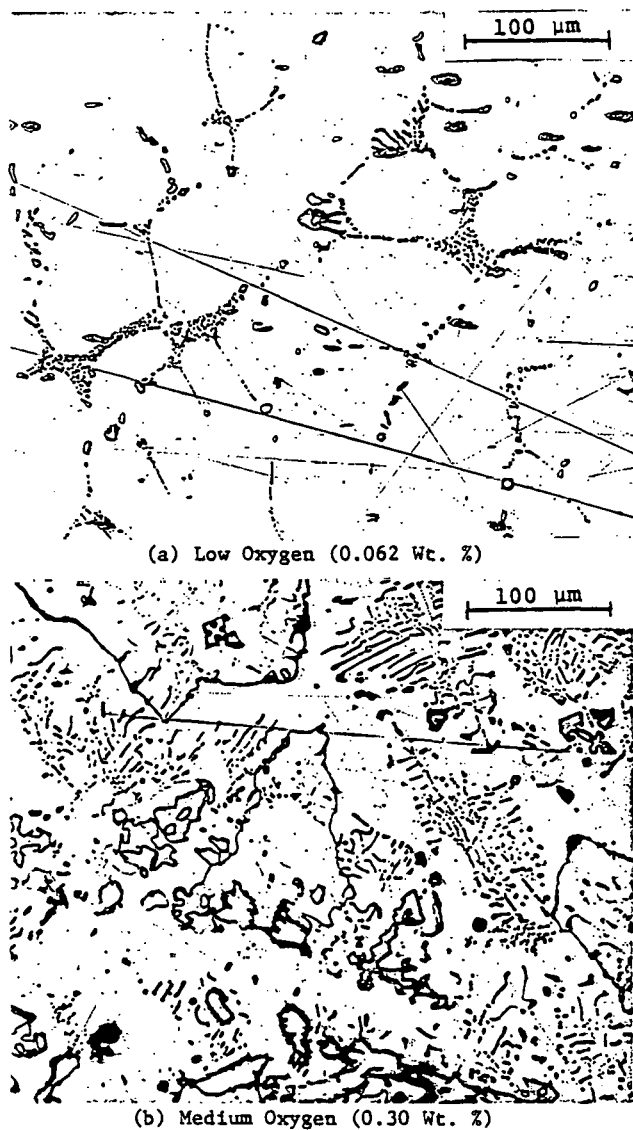


Figure 3 - Effect of O-Content on the As-Cast Microstructure of FeTi

but for practical purposes $\text{Fe}_7\text{Ti}_{10}\text{O}_3$ may be considered the predominant phase resulting from O-contamination. This phase is crystallographically identical to that reported recently by Pick and Wenzl in O-contaminated FeTi[7]. In fact, this phase has been reported at least twice before in the Fe-Ti-O system under the designation T-phase ($\text{Ti}_4\text{Fe}_2\text{O}-\text{Ti}_3\text{Fe}_2\text{O}$)[10,11] or the ϵ Fe-Ti-O phase (O-stabilized Ti_2Fe)[12]. The phase is not strictly an oxide but rather a classic "oxygen-stabilized" intermetallic compound; i.e., an intermetallic that does not appear in the pure metal binary phase diagram (Figure 1) but is electronically stabilized by oxygen[13].

$\text{Fe}_7\text{Ti}_{10}\text{O}_3$ is present as a solidification product down to very low oxygen levels, at least down to 0.01 wt. % (100 ppm) oxygen, the lowest-oxygen sample prepared. Thus it is apparent that while the solubility for oxygen in liquid FeTi is high (at least 1 wt. %), solid FeTi has almost zero solubility for oxygen. Therefore, essentially all of the oxygen is rejected as the $\text{Fe}_7\text{Ti}_{10}\text{O}_3$ phase during solidification. Because each O-atom

ties up 5.7 metal atoms, the effect of this is substantial on the hydrogen storage capacity. From the stoichiometry of $\text{Fe}_7\text{Ti}_{10}\text{O}_3$, 1 wt. % O-contamination in the alloy would be expected to result in about 19 wt. % $\text{Fe}_7\text{Ti}_{10}\text{O}_3$ phase. We have seen no evidence that this phase can be hydrided, at least at temperatures and H_2 pressures used for FeTi (Pick and Wenzl came to the same conclusion[7]). Thus O-contamination dilutes the FeTi phase with substantial amounts of useless $\text{Fe}_7\text{Ti}_{10}\text{O}_3$. As shown in Figure 4, the actual dilution effect

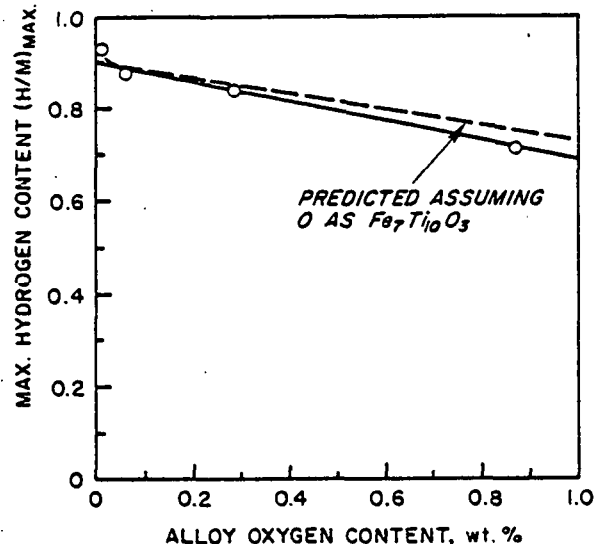


FIGURE 4-EFFECT OF FeTi OXYGEN CONTENT ON THE MAXIMUM HYDRIDING CAPACITY. $T=40^\circ\text{C}$, $P=68\text{ ATM}$ (6.9 MPa)

measured as a loss of hydrogen capacity with O-contamination corresponds closely to that predicted by $\text{Fe}_7\text{Ti}_{10}\text{O}_3$ formation. In view of the effect of oxygen, production practices should obviously consider means to prepare FeTi with O-contents as low as practical within reasonable economic constraints.

The effect of the other two common melting contaminants carbon and nitrogen should be briefly considered. Carbon is a tramp element incurred from the use of carbon-steel as a raw material for FeTi production. In FeTi we find the carbon partitions in the form of very stable Ti-rich carbides, essentially TiC. The TiC particles do not hydride. Because each carbon-atom ties up only one metal atom, the deleterious effect of a given level C-contamination on hydrogen capacity is much less than the same amount of O-contamination. However, if fairly high-C steel (say >0.5%) is used, a slightly higher Ti charge should be used to compensate for the Ti lost in TiC formation. Although we do not have a complete story on the effect of N-contamination (e.g., during air melting) it appears to be relatively harmless and probably plays a role similar to carbon in forming a small amount of TiN or Ti(C,N) in the microstructure.

ACTIVATION

Virgin FeTi does not hydride on contact with high pressure H_2 at room temperature. It must be "activated". Activation is a term meaning to

establish complete hydriding of a sample for the first time and consists of two distinct stages: (1) the initiation of some initial hydrogen absorption on particle surfaces, which can be achieved by heating the sample to a few hundred degrees C under vacuum and then exposing it to a small pressure of H_2 gas, and (2) the propagation of the hydride throughout the particles at ambient temperatures under substantial pressures of H_2 . We now present observations concerning each of these stages.

The first stage of activation is not very well understood. Unlike Ni, La, FeTi will not activate upon first exposure to high pressure, room temperature H_2 . By Auger spectroscopy of the surface chemistry of FeTi crushed in air, we know that each particle is enveloped by a thin (roughly 200-300 Å thick) oxygen-rich film. Whether this film is an oxide, suboxide, or merely adsorbed oxygen is not known. In any event it is an apparent barrier that prevents hydrogen from reacting at room temperature with the metal substrate. By following the above procedure, the film is somehow made transparent to hydrogen or removed, so that some absorption into the metal occurs. Although it seems thermodynamically unlikely that a Ti-rich oxide would be reduced by H_2 at such low temperatures[14], the process does at least partially disrupt the film so that the sample will continue to absorb hydrogen when cooled to room temperature. The first stage of the activation occurs quite easily (as long as adequate purity H_2 is used) and seems to be fairly insensitive to the microstructure of the FeTi. If the activated alloy is exposed to air or impure H_2 , the O-rich film will reform, requiring the first stage activation procedure to be repeated.

The second stage of the activation (i.e., the conversion of the entire sample to hydride at room temperature) is very dependent on the alloy microstructure. For 30-50 mesh (600-300μm) particles, activation can be completed in times as short as 2 hours or as long as two weeks. In general, the smaller the amount of second phases present in the alloy (i.e., the higher the purity), the slower is the second stage activation. Figure 5 shows the

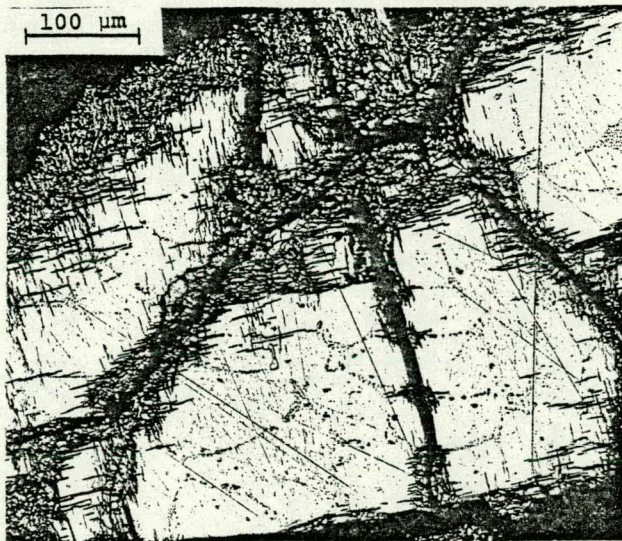


Figure 5 - Partially Hydrided Particle of Low-O (0.062 Wt. %) FeTi

microstructure of a partially hydrided particle of high purity (0.062 wt. %) FeTi. The hydride initially grows as an envelope about the particle with the hydride penetrating as a series of fine platelets, usually orthogonal in morphology. Because there is a 10% volume increase on hydriding, the growing hydride envelope exerts stresses on the remaining unhydrided core. The FeTi alloy is fairly brittle and occasionally cracks, forming new surfaces for hydriding. Several of these major cracks have occurred at various times in the particle of Figure 5. Occasional cycling of the sample (dehydriding followed by rehydriding) helps to aid the cracking required for second stage activation.

Second phase particles seem to promote activation in two ways: (a) they lower the fracture toughness of FeTi (i.e., increase its brittleness) thus making the major activation cracks easier to form and propagate, and (b) they provide interfaces for preferential hydride nucleation and penetration. The sample shown in Figure 5 was activating very slowly. This sample was of low oxygen content and a relatively clean microstructure (Figure 3a). In contrast, a partially hydrided particle of higher oxygen content FeTi is shown in Figure 6 (the

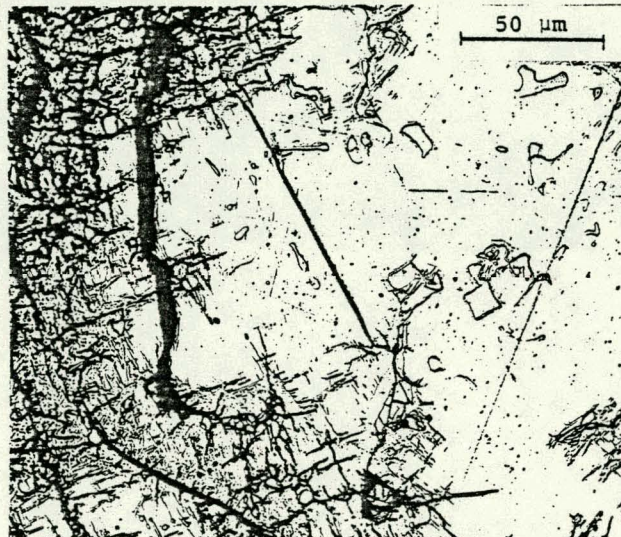


Figure 6 - Partially Hydrided Particle of Medium-O (0.30 Wt. %) FeTi

alloy microstructure of this sample is shown in Figure 3b). The medium oxygen sample was much easier to activate. Preferential cracking and hydride penetration can be seen along the numerous $Fe_3Ti_{10}O_3$ and occasional Fe_2Ti particles in Figure 6.

Thus the manipulation of alloy microstructure can be an important tool in controlling the ease of second stage activation. $Fe_3Ti_{10}O_3$ and Fe_2Ti particles promote activation. Also we find that small amounts of excess Ti solid solution in the microstructure dramatically increases activation rate with rapid initial penetration of the hydride along continuous or semi-continuous networks of this phase. Fine grain size is also helpful in aiding activation although its effect is not as dramatic as that of the second phases discussed above. Unfortunately, as pointed out earlier, $Fe_3Ti_{10}O_3$, Fe_2Ti , and free Ti solid solution all decrease the storage capacity of FeTi alloys. A

future challenge in microstructural design would be to develop a two-phase FeTi + X microstructure that would promote activation without seriously reducing storage capacity (i.e., a small amount of X).

DECREPITATION (PARTICLE SIZE BREAKDOWN)

In practice virgin FeTi is usually crushed to a particle size on the order of 10-50 mesh (2-0.3 mm) before use. After a number of hydriding/dehydriding cycles the apparent particle size (as measured by a screen analysis, for example) is seen to decrease. This has practical implications in bed design as to packing, H₂ permeation, heat transfer, etc. Here we present some microstructural observations of this phenomenon and how it might be controlled.

The microstructure of a high purity (0.038%) FeTi sample after a few hydriding cycles, followed by complete dehydriding is shown in Figure 7.

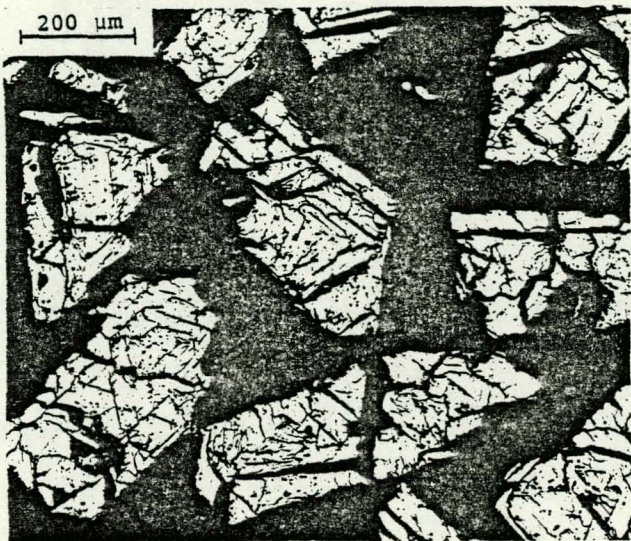


Figure 7 - Particles of Low-O (0.038 Wt. %) FeTi After 15 Hydriding/Dehydriding Cycles. Unetched

Before hydriding the sample had been crushed to -30, +50 mesh (600-300 μm). The particles shown in Figure 7 are largely the same overall size as before hydriding. However they are highly cracked. There are two size scales for the cracks: (a) a series of coarse blocky cracks that are the remnants of the major activation cracks noted earlier (Figure 5) and (b) a series of much finer cracks down to a scale of 2-10 μm. All of these cracks, of course, result from stresses imposed from the volume changes during hydriding and dehydriding. Such a highly cracked structure is ideal from a surface area and reaction kinetics point of view. The problem is that repeated cycling causes the fragments of the highly cracked aggregates to detach, resulting in a range of effective particle sizes and hence packing. Because each highly cracked aggregate is very fragile, physical vibrations probably contribute as much to decrepitation as the hydriding reaction itself. The initial detachments that occur are the relatively coarse blocks. Some of these can be seen partially detached in Figure 7. The finer (2-10 μm) fragments are much more interlocked and resistant

to detachment. Except for detachment and separation of some of the already cracked fragments, the microstructure of a sample cycled several thousand times is really little different from one cycled only a few times.

In view of the observations made on activation it might be expected that decrepitation would be a function of virgin alloy microstructure. This is the case. The medium-oxygen alloy shown in Figure 3b (easy to activate) was subject to more pronounced decrepitation with cycling than the low-oxygen sample shown in Figure 3a (hard to activate). For example, starting with -10, +16 mesh (2000-1800 μm) medium-oxygen material, 1500 cycles resulted in enough decrepitation such that 49% of the sample passed through a 400 mesh (38 μm) screen. In comparison, a similar sample of the low-oxygen FeTi after 5500 cycles resulted in only 8% of the sample being small enough to pass through a 325 mesh (45 μm) screen. This trend is likely a direct result of the effect of Fe₇Ti₁₀O₃ particles in lowering the fracture toughness of FeTi and contributing to the coarse activation crack pattern. Other phases seem to have strong effects. For example, depending on the amount and distribution, excess Ti solid solution can promote a finer activation crack size. In addition, the partial substitution of other elements such as manganese or nickel seem to affect the crack patterns in ways not yet fully understood. In summary, microstructure control provides the alloy designer with a potential tool to control the decrepitation phenomenon in FeTi.

HYDRIDE STABILITY

Recently Reilly and Johnson have demonstrated a greatly increased versatility for FeTi by substituting various ternary transition elements into the alloy[15]. The shape of pressure-composition isotherms and the level of the plateau (i.e., the stability of the hydride) can be varied substantially. A few examples of modified alloys are shown in Figure 8. In this section we briefly discuss these effects in terms of bonding changes and resultant effects on the FeTi crystal structure.

Figure 9 shows the crystal structure of FeTi. It is the so-called B2 or CsCl structure, the most common structure encountered for equiatomic intermetallic compounds[13]. It is a body-centered-cubic lattice with Ti atoms located on the corners of the unit cell and an Fe atom in the center (or vice versa). Dimensionally it is described by the single lattice parameter a_0 . It is possible to at least partially substitute other elements such as manganese, chromium, nickel and vanadium into the FeTi lattice and it is this substitution that modifies the stability of the subsequent hydride. In all cases the stability was increased; i.e., the lower plateau level was decreased in Figure 8 from the reference FeTi level. A large number of precision lattice parameter measurements were made on ternary Ti_{1-x}My phases and correlated with the 40°C plateau level (or rather more roughly the dissociation pressure at H/M = 0.4 since in many cases the ternary alloys do not show a level plateau). The correlation is shown in Figure 10. Although there is scatter of the data, it is clearly evident that increases in hydride stability resulting from substitution of ternary elements are accompanied by increases in the lattice parameter of the Ti_{1-x}My phase.

The effect shown in Figure 10 can, at least in

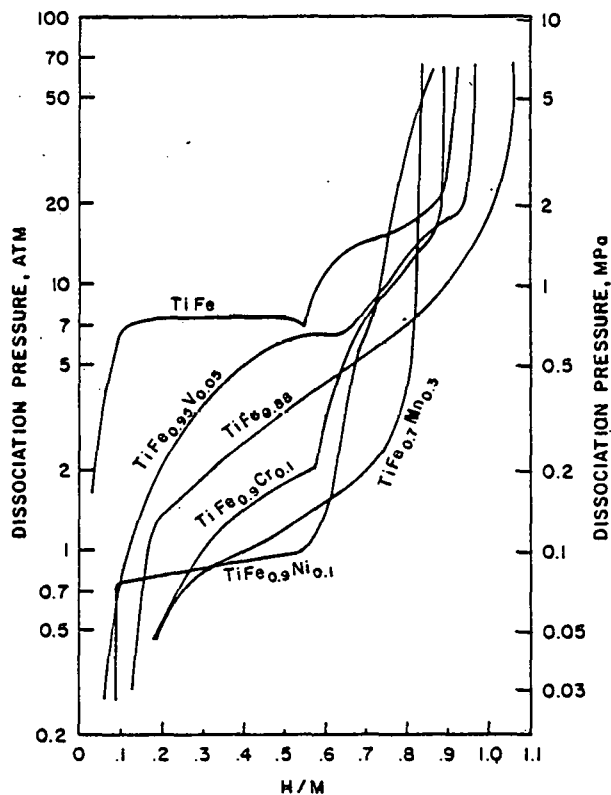


FIGURE 8 - EFFECT OF VARIOUS TRANSITION METAL SUBSTITUTIONS ON THE 40°C DESORPTION ISOTHERM.

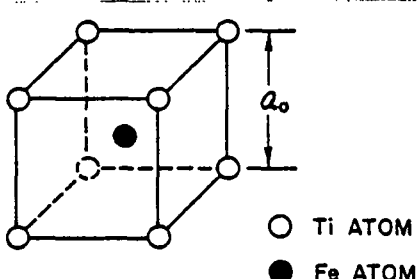


FIGURE 9 - CRYSTAL STRUCTURE OF FeTi.

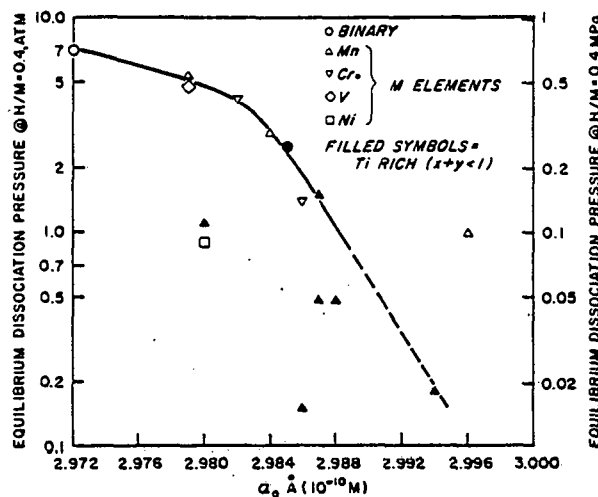


FIGURE 10 - CORRELATION BETWEEN DISSOCIATION PRESSURE AND LATTICE PARAMETER OF $TiFe_xM_y$ ALLOYS.

a qualitative sense, be interpreted in terms of interatomic bonding. For $FeTi$, the lattice parameter is considerably smaller than would be predicted by packing of neutral Ti and Fe alloys in a $CsCl$ lattice array. This "lattice contraction" is taken as an indication of substantial ionic bonding in $FeTi$ [13]. Ti enrichment or substitution of ternary elements such as manganese, chromium, nickel or vanadium, increases the lattice parameter, thus decreasing the "lattice contraction" or decreasing the overall bond strength. This apparently results in a more stable hydride (i.e., a lower plateau level). The situation seems roughly analogous to the "Rule of Reversed Stability" observed by van Mal, et al for nickel-rare earth hydrides[16], which states qualitatively that the more stable the intermetallic compound the less stable is its hydride.

The rough correlation between plateau level and metal lattice parameter should serve as a convenient tool for alloy screening. As a caution on Figure 10, it should be noted that those points falling below about 0.5 atm (0.05 MPa) should be considered approximate since the reversible range for these alloys was narrow due to an excess of free Ti in the microstructure.

Manganese is the most cost effective additive for manipulation of the hydriding behavior. Manganese shifts the homogeneity range of $FeTi$ slightly toward the Ti -rich end [i.e., simple substitution of Mn for some of the Fe results in some $(Fe,Mn)_2Ti$ in the microstructure]. Work is continuing on optimizing the $Ti-Fe-Mn$ system using the metallurgical tools developed thus far in this work.

CONCLUDING REMARKS

In this paper we have shown that, in spite of its simple formula, $FeTi$ is metallurgically quite complex. Economically and technically effective production and use of $Fe-Ti$ alloys for hydrogen storage requires an adequate understanding of the metallurgy of the alloys and the interrelations between microstructure and hydriding behavior. Within the complexity of the system lies an inherent versatility and future efforts should provide a wide range of properties to suit a variety of potential mobile and stationary hydrogen storage applications.

ACKNOWLEDGEMENTS

This work was performed under the support of the U.S. Energy Research and Development Administration, by subcontract to Brookhaven National Labs, and The International Nickel Company, Inc.

REFERENCES

1. Reilly, J.J. and Wiswall, R.H., Jr., "Formation and Properties of Iron Titanium Hydride", *Inorganic Chem.*, 13, 218 (1974).
2. Billings, R.E., "Hydrogen Storage in Automobiles Using Cryogenics and Metal Hydrides", *Proc. The Hydrogen Economy Miami Energy (THEME) Conf.*, S8-51, Miami Beach, 1974.
3. Henriksen, D.L., Mackay, D.B., and Anderson, V.R., "Prototype Hydrogen Automobile Using a Metal Hydride", *Proc. 1st World Hydrogen Energy Conf.*, III, 7C-1, Miami Beach, 1976.
4. Billings, R.E., "A Hydrogen-Powered Mass Transit System", *Proc. 1st World Hydrogen Energy Conf.*, III, 7C-27, Miami Beach, 1976.
5. Buchner, A. and Saufferer, H., "The Short and Medium Term Development and Practical Application of Hydrogen-Powered Vehicles", *2nd Symposium on Low Pollution Power Systems Development*, Dusseldorf, 1975.
6. Burger, J.M., Lewis, P.A., Isler, R.J., Salzano, F.J. and King, J.M., "Energy Storage for Utilities Via Hydrogen Systems", *Proc. 9th IECEC*, 428, San Francisco, 1974.
7. Pick, M.A. and Wenzl, H., "Physical Metallurgy of FeTi-Hydride and Its Behavior in a Hydrogen Storage Container", *Proc. 1st World Hydrogen Energy Conf.*, II, 8B-27, Miami Beach, 1976.
8. Sandrock, G.D., "The Interrelations Among Composition, Microstructure and Hydriding Behavior for Alloys Based on the Intermetallic Compound FeTi", *The International Nickel Company, Inc., Final Report under Contract BNL 35241OS*, in preparation.
9. Lyman, T., *Editor, Metals Handbook*, Vol. 8, American Society for Metals, Metals Park, OH, 1973, p. 307.
10. Rostoker, W., "Observations on the Occurrence of Ti_2X Phases", *Trans. AIME*, 194, 209 (1952).
11. Rostoker, W., "Selected Isothermal Sections in the Titanium-Rich Corners of the Systems Ti-Fe-O, Ti-Cr-O, and Ti-Ni-O", *Trans. AIME*, 203, 113 (1955).
12. Ence, E. and Margolin, H., "Re-Examination of Ti-Fe and Ti-Fe-O Phase Relations", *Trans. AIME*, 206, 572 (1956).
13. Nevitt, M.V., "Alloy Chemistry of Transition Elements", *Electronic Structural and Alloy Chemistry of the Transition Elements*, (P.A. Beck, Ed.), Interscience, NY, 1963, pp. 101-178.
14. Darken, L.S. and Curry, R.W., *Physical Chemistry of Metals*, McGraw-Hill, NY, 1953, p. 349.
15. Reilly, J.J. and Johnson, J.R., "Titanium Alloy Hydrides; Their Properties and Applications", *Proc. 1st World Hydrogen Energy Conf.*, II, 8B-3, Miami Beach, 1976.
16. van Mal, H.H., Buschow, K.H.J. and Miedema, A.R., "Hydrogen Absorption in $LaNi_3$ and Related Compounds: Experimental Observations and Their Explanation", *J. Less Common Metals*, 35, 65 (1974).